Article

Annual Thermal Management of the Photovoltaic Module to Enhance Electrical Power and Efficiency Using Heat Batteries

Prasannaa Poongavanam [1] , Aneesh A. Chand [2,*] , Van Ba Tai [3], Yash Munnalal Gupta [4,*],
Madhan Kuppusamy [5] , Joshuva Arockia Dhanraj [6] , Karthikeyan Velmurugan [7,8,*], Rajasekar Rajagopal [9] ,
Tholkappiyan Ramachandran [10] , Kushal A. Prasad [2] , Shyamal Shivneel Chand [2] , Shivnesh Raj [2]
and Kabir A. Mamun [2]

1. Department of Mechanical Engineering, Annamalai University, Chidambaram 608002, Tamil Nadu, India;
    prasannaina@gmail.com
2. School of Information Technology, Engineering, Mathematics and Physics (STEMP),
    The University of the South Pacific, Suva, Fiji; kushalaniketp@gmail.com (K.A.P.);
    chand97shyamal@gmail.com (S.S.C.); rajshivnesh2@gmail.com (S.R.); kabir.mamun@usp.ac.fj (K.A.M.)
3. Faculty of Technology, Dong Nai Technology University, Bien Hoa 76000, Dong Nai, Vietnam;
    vanbatai@dntu.edu.vn
4. Department of Biology, Faculty of Science, Naresuan University, 99 Moo 9 Phitsanulok-Nakhonsawan Road,
    Phitsanulok 65000, Thailand
5. GOONWORLD Corporate Research Institute, Dong-gu Inovalley 26 Road 9-115,
    Daegu 11051, Republic of Korea; mitmadhan@gmail.com
6. Centre for Automation and Robotics (ANRO), Department of Mechatronics Engineering,
    Hindustan Institute of Technology and Science, Padur, Chennai 603103, Tamil Nadu, India;
    joshuva1991@gmail.com
7. Center for Alternative Energy Research and Development, Khon Kaen University, Khon Kaen 40002, Thailand
8. Mechanical Engineering Division, Faculty of Engineering, Khon Kaen University, Khon Kaen 40002, Thailand
9. Department of Mechanical Engineering, Saveetha Engineering College, Chennai 602105, Tamil Nadu, India;
    rajeee.mech@gmail.com
10. Department of Physics, College of Science, United Arab Emirates University, Al Ain P.O. Box No. 15551,
    United Arab Emirates; thols2006@gmail.com
*   Correspondence: aneeshamitesh@gmail.com (A.A.C.); yashmunnalalg@nu.ac.th (Y.M.G.);
    karthi230407@gmail.com (K.V.)

Abstract: Several studies state that phase change material (PCM) improves the electrical power and efficiency of the photovoltaic (PV) module. To find the suitable PCM for tropical climatic conditions, multi-PCMs are examined simultaneously with melting temperatures of 31 °C, 35 °C, 37 °C, and 42 °C. In this study, PCM containers are integrated behind the PV module with a thickness of 50 mm. The performance of the multi PV-PCMs is monitored year-round and compared with PV-noPCM. The experimental results show that the selected four PCMs performed the cooling process autonomously in all the climates, such as PCM with a melting temperature of 37 °C and 42 °C enhanced the higher cooling rate in summer, and the same PCMs failed to achieve a higher cooling rate in winter. The lowest temperature drop was noted for pre-monsoon and monsoon seasons due to the low irradiance. On the other hand, the highest temperature drop of 16.33 °C is observed for pre-summer (March) and 15.7 °C, and 17.14 °C for summer (April) as compared to PV-noPCM. The results of the present investigation highlight the requirement for choosing the proper PCM melting temperature based on optimal year-round performance. Further, it is recommended that a single PCM melting temperature for cooling the PV modules year-round in tropical climates is inappropriate, and instead, a cascaded structure with different PCM melting temperatures is recommended.

Keywords: multi-PCM; heat batteries; annual cooling; power enhancement

1. Introduction

An increase in global energy demand widely increased fossil fuel consumption, resulting in the depletion of the ozone layer and the rise of environmental pollution [1–3]. Several studies show that producing electrical energy using sustainable methods could minimize human-made disasters and healthy lifestyles for future generations [4,5]. A solar photovoltaic (PV) system plays a dominant role in the energy market; however, its internal loss restricts the operation of the power plant [6,7]. Solar farms have undergone several losses among the rise in the PV module operating temperature becomes a greater threat to the power production and lifetime of the solar farm [8]. Reducing the temperature of the PV module enhances the voltage profile resulting in higher power and efficiency attained [9]. In the past, sensible heat storage materials have been widely employed to remove the excess heat from the PV module, specifically, water sprayed over the PV module's glass surface [10,11]. Considering the thermal load requirements for low and midsized commercial applications, water channels are attached behind the PV module to utilize the hot water [12,13]. In subtropical conditions, air flows in the front and back surface of the PV module for room heating purposes [14], and depending on the application, working fluids are alternatively changed and the excess heat is utilized for useful applications and also to improve electrical power production [15]. The above-mentioned methods are mostly operated by an active method because passive techniques using water and air are not effective due to the low specific heat capacity of the materials [16]. However, the active method consumes external power sources, and adequate maintenance is required which makes the entire system complex [17]. To overcome this issue, phase change material (PCM) is widely used as an alternative to water- and air-based cooling techniques [18,19]. Comparatively, PCM-specific heat capacity is lower than water; however, PCM dominates the cooling operation as PCM stores the heat energy using latent heat of fusion (H_m) [20]. During the solid and liquid state, the performance of PCM is lower than water and air; notably, during the melting state PCM stores the heat energy in higher order (J/g) as compared to sensible heat storage materials (J/g·K) [21,22].

In the past two decades, PCM gained popularity in storing heat energy and is often called heat batteries [19,23]. Particularly for cooling the PV module, PCMs are attached behind the PV module to remove the excess heat and it naturally dissipates the heat energy to the surroundings [24,25]. PCM changes its phase during the charging and discharging period, considering its phase-changing property. PCMs are often filled in a container to avoid PCM leakage [26,27]. To avoid the complexity of PCM container fabrication, Jae-Han Lim et al. [28] filled the solid PCM in a plastic bag and attached it with a PV module. During the sunshine, PCM absorbs the heat energy from the PV module, but it is not effective as compared to metal containers. The thermal conductivity of the plastic bag is less than a metal-based PCM container, resulting in thermal resistance increased between the PV module and PCM. Several studies reported that metal-based PCM containers increased the heat transfer rate and enhanced the cooling rate in higher order [29,30]. Notably, the decrease in thickness of PCM container material decreases the conduction resistance between the PV module and PCM but low thickness PCM container material failed to maintain the smooth surface. An uneven PCM container surface creates contact resistance and reduces the heat transfer rate, resulting in lower cooling achieved. To avoid contact resistance, PCMs are filled over the tedlar surface whereas the PCM gains heat energy without using a secondary layer between the PV module and PCM [31]. This technique improves the cooling rate; however, it is hard to enclose the sides and back surfaces of the PCM. Secondly, due to low PCM thermal conductivity (0.2–0.3 W/m·K), there have been struggles to store and discharge the heat energy in an efficient way, resulting in the H_m of the PCM not being utilized effectively [32–34]. Velmurugan et al. developed a composite PCM using expanded graphite (EG) to increase the thermal conductivity of the PCM. Comparatively, prepared composite PCM enabled the cooling effect as compared to pure PCM [35]. Further, several studies reported that thermal conductivity-enhanced PCM exhibits higher cooling and faster discharging during the non-sunshine hours which

favors resuming the cooling process for a consecutive day [36,37]. The above-mentioned contact resistance and low thermal conductivity resistance are common in designing the PCM as a cooling agent and it is necessary to consider them for effective cooling. Apart from these issues, several researchers stated that PCM melting temperature is the major concern in cooling the PV module [38]. As mentioned earlier, PCMs are latent heat storage materials, and they store heat energy in the form of H_m which will be activated during the PCM melting. If the selected PCM does not reach the melting temperature during the effective sunshine hours, PCM is not capable of cooling the PV module effectively and, under certain conditions, an inappropriate PCM melting temperature is adverse to the PV module operations and increases the PV module operating temperature higher than the unmodified or uncooled PV module [39]. Notably, the PV module operates in the range of 60–80 °C under tropical conditions and the operating temperature of the PV module is highly correlated with environmental factors such as solar irradiance, wind speed, humidity, ambient temperature, atmospheric pressure, and other parameters [40,41]. All these parameters are unpredictable for annual PV module cooling; for example, selected PCM can reduce the PV module operating temperature higher in summer, and in winter it will not be effective due to the variation in the environmental factors that affect the operation of the PCM as a cooling agent for the PV module [27,42]. Several studies suggest performing the theoretical simulation to minimize the uncertainty in the experiment; however, it is difficult to include all the above-mentioned environmental factors in the simulation. Considering these complications, in this study, four different types of PCMs are examined under tropical climatic conditions of Chidambaram, Tamil Nadu, India to find the relationship of the PCM operation in cooling the PV module. All the PCMs are examined under outdoor climatic conditions for twelve months to find the reliability of PCM in cooling the PV module. Further, comparative studies are performed between the summer, winter, and monsoon seasons for all four PCMs to recommend the suitable PCM for large-scale solar farms.

2. Materials and Methods

2.1. Materials

In this study, four different melting temperature PCMs are purchased from Pluss Advanced Technologies Pvt. Ltd., Haryana, India. Further, without undergoing any chemical treatment, purchased commercial PCMs are utilized for cooling the PV module. Thermophysical properties of the commercial PCMs are listed in Table 1 [43].

Table 1. Thermophysical properties of the commercial PCMs.

PCM	OM31 (PCM1)	OM35 (PCM2)	OM37 (PCM3)	OM42 (PCM4)
Melting temperature (°C)	32	35	37	42
Latent heat of fusion (J/k)	187	202	218	199
Thermal conductivity (W/m·K)	0.21	0.20	0.16	0.19

2.2. Experimental Setup

PV module cooling's performed under real-time operating conditions at Chidambaram, Tamil Nadu, India (11.39° N, 79.70° E). A total of five polycrystalline PV modules are used in this study (Table 2); the first PV module is unmodified and considered a reference system, and the remaining four PV modules are integrated with a 5 cm thickness (23 cm ×13.6 cm × 5 cm (L × W × H)) = 1.372 kg) of PCM1, PCM2, PCM3, and PCM4 respectively as shown in Figure 1. Considering the phase-changing property of the PCM, a 2 mm thickness of the aluminum sheet is used to fabricate the PCM container and 20% of the PCM container volume is kept empty for PCM volume expansion. PCM-filled containers are directly integrated behind the PV module back surface without using any heat-conductive materials. The reason behind the direct integration of the PCM container is to avoid resistance in heat transfer and the surface of the PCM container contains high

thermal conductivity (247 W/m·K) which helps to transfer the heat from the PV module to the PCM in a faster way. To make the comparative study, five PV modules (with and without PCM containers) were examined simultaneously. During the experimentation period, PV module operating temperatures are measured using K-type thermocouples at an interval of 15 min. Considering the examined 5 Wp polycrystalline PV module surface area, a single K-type thermocouple is placed at the center part of each PV module's front surface considering the hottest area [27]. Following that, the ambient temperature is measured using the sixth K-type thermocouple at the experimental site. Table 3 shows the experimental device measurement range and accuracy and the corresponding voltage and current profiles are recorded to calculate the maximum power, performance ratio (PR), efficiency (η), and capacity utilization factor using Equations (1)–(4), respectively.

Table 2. PV module specification.

Specification	Range
Rated power (P_{max})	5 W
Open circuit voltage (V_{oc})	22.3 V
Short circuit current (I_{sc})	0.3 A
Electrical efficiency (η_{elc})	11.5%
Voltage at P_{max} (v_{vmp})	17.8 V
Current at P_{max} (I_{mp})	0.28 A
Temperature co-efficient (β)	−0.45%/°C
Dimension (L × W)	30 cm × 20 cm

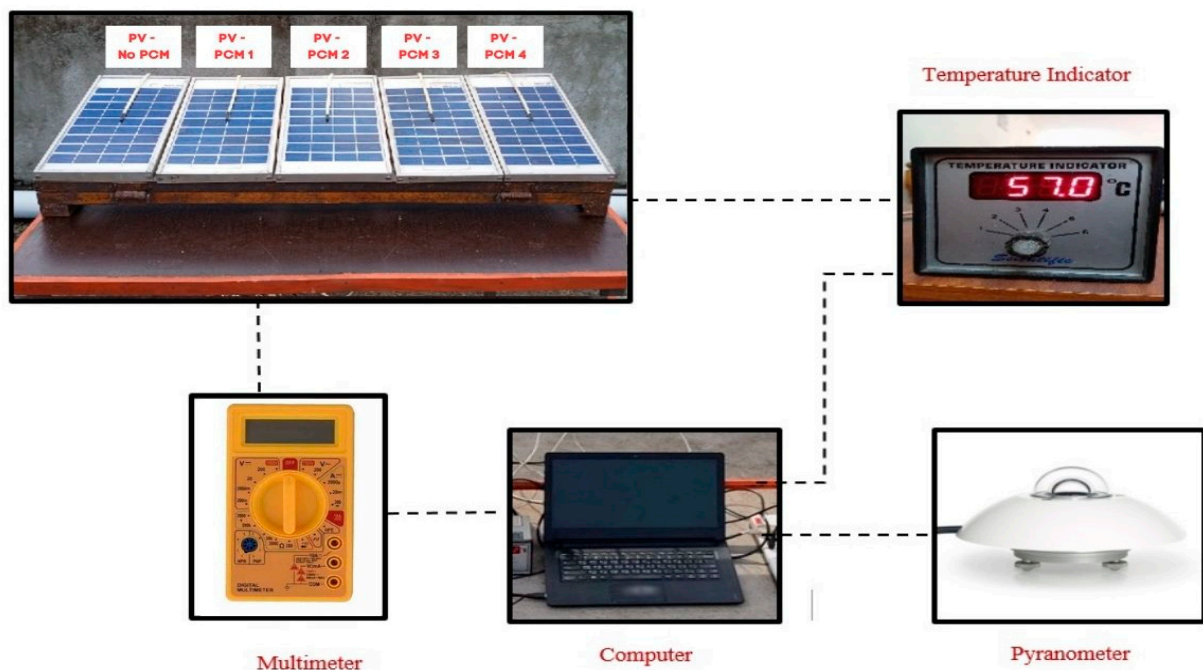**Figure 1.** Schematic view of an experimental setup.

Table 3. Measuring device range and accuracy.

Device Name	Range	Accuracy
K-type thermocouple	−270 to 1370 °C	±0.30%
Multimeter	200 mV to 1000 V, 200 μA to 10 A	±1.3%
Pyranometer	0 to 1600 W/m^2	±0.25%
Temperature indicator	−50 to 400 °C	±1.1%

A solar cell is a current generator, an increase in solar irradiance generates a higher current than voltage; however, the product of maximum current with the voltage produces the maximum power.

$$Maximum\ power\ =\ maximum\ voltage\ \times\ maximum\ current \tag{1}$$

The performance ratio is generally used in large-scale solar farms to evaluate the long-term performance of the system.

$$PR\ =\ \frac{PV\ power\ generation}{Installed\ capacity\ \times\ \frac{Solar\ irradiance}{1000}}\ \times\ 100 \tag{2}$$

The efficiency of the solar *PV* modules is widely calculated to find the output of the system following the received input as solar irradiance.

$$Efficiency\ (\eta) = \eta_{elc}\left(1 - \beta\left(T_{PV} - T_{ref}\right)\right) \tag{3}$$

where η obtained efficiency under real-time operating conditions, η_{elc} is the manufacturer-rated efficiency under STC, β is the temperature coefficient, T_{PV} is the real-time PV module operating temperature, and T_{ref} is the PV module operating temperature at STC.

The capacity utilization factor is mainly used to evaluate the annual performance of the solar *PV* system.

$$CUF = \frac{Annual\ energy}{Day \times 24\,\text{h} \times installed\ capacity}\ \times\ 100 \tag{4}$$

3. Results

3.1. PV Module Thermal Profile Using PCMs

3.1.1. Pre-Summer

Cooling the PV module over the raise in the PV module operating temperature will improve the voltage and current production. It is noted that during the summer, the PV module temperature rises abruptly; however, under tropical locations, a non-summer period also requires the cooling system to obtain a higher efficiency and performance ratio. During March, the experimental location's ambient temperature started raising higher than 30 °C at the experimentation starting period and reached the peak ambient temperature of 33.91 °C. The rise in ambient temperature is highly correlated with the rise in PV module temperature as compared to solar irradiance and other environmental factors [18]. Figure 2 shows the overall performance of the PV module operations using four different PCM melting temperatures. Owing to the effective solar irradiance, the ambient temperature rose higher than in winter, resulting in the PV module operating temperature reaching a peak of 66.17 °C. At the starting period of experimentation, the PV-noPCM operating temperature was sustained at 45 °C and the corresponding PCM1-, PCM2-, PCM3-, and PCM4-assisted PV module operating temperatures were maintained at 34.1 °C, 35.8 °C, 36.4 °C, and 39.1 °C, respectively. Notably, PCM1 maintained a lower operating temperature than other PCMs and PCM4 maintained a higher operating temperature; however, it is lower than PV-noPCM. Considering the low melting temperature of PCM1, the early period of the experiment enhanced effective cooling and PV-PCM4 exhibits lower cooling due to the high melting temperature. A further increase in solar irradiance delivers higher PV module operating temperatures; during 09:30, PV-noPCM temperature reached 57.46 °C and, notably, PV-PCM1, PV-PCM2, PV-PCM3, and PV-PCM4 operating temperatures reached 48.52 °C, 47.02 °C, 44.34 °C, and 45.01 °C, respectively. The PV-PCM1 cooling effect started declining due to the liquefaction of PCM at an early stage of experimentation. It is found that lower PCM melting temperatures are not suitable for non-winter conditions. Further, throughout the experimentation period, PCM1-assisted PV module operating temperature is higher than other PCMs and, beneficially, it is noted

that PCM4 maintained a maximum of 16.34 °C lower than PV-noPCM which is the highest cooling rate as compared to other PCMs. However, a similar operation was achieved for PCM3 following PCM4. It is concluded that for pre-summer climatic conditions, PCM4 and PCM3 are suitable for cooling the excess rise in the PV module temperature.
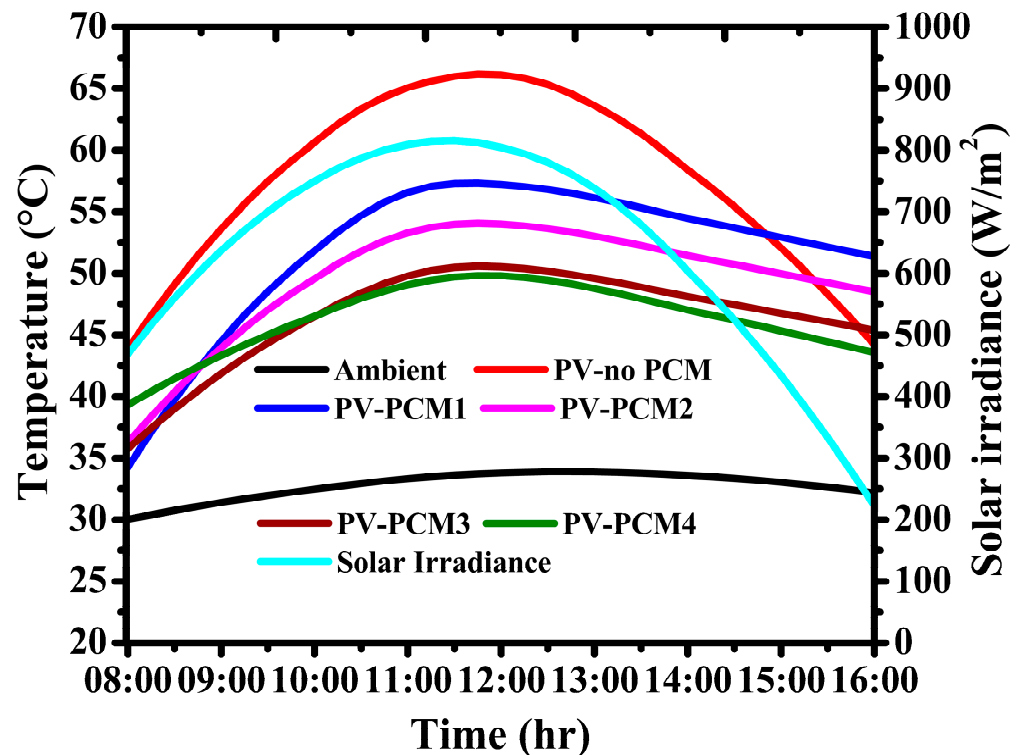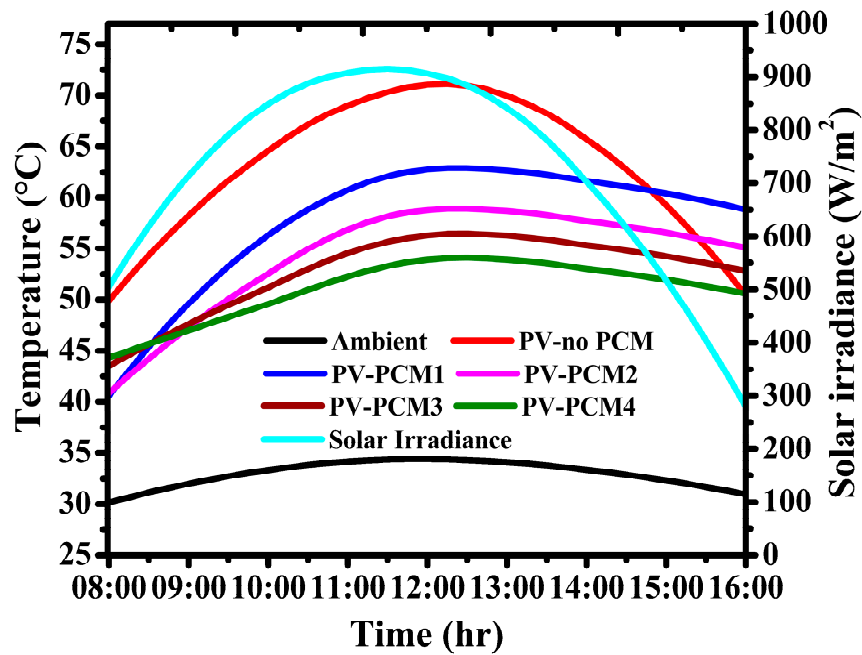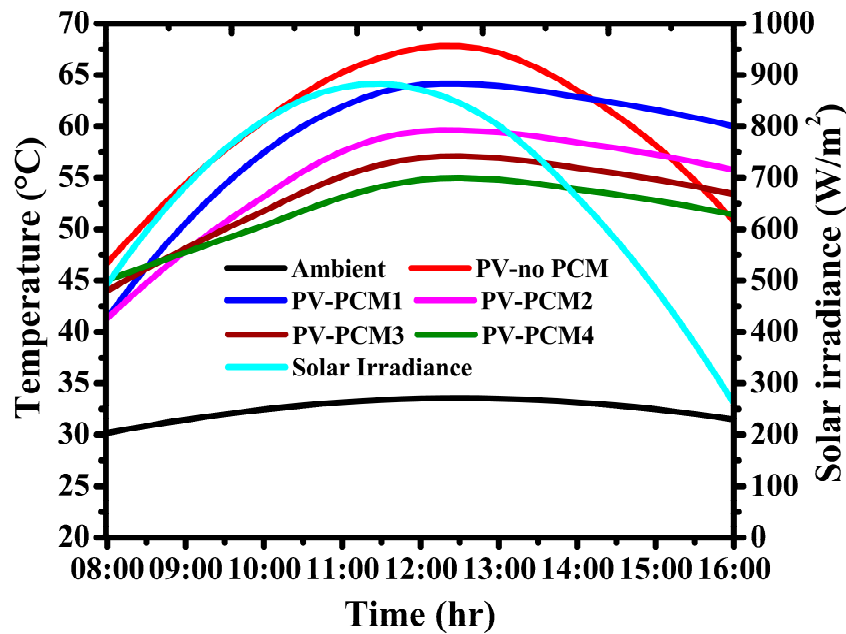

Figure 2. Solar irradiance and thermal profile of PV with and without PCM (March).

3.1.2. Summer

Figure 3 shows the meteorological and PV module thermal profiles under summer climatic conditions. For the experimental location, April and May are considered summer periods owing to the higher ambient temperature of 34.39 °C and 33.57 °C, as shown in Figure 3a,b, respectively. April average solar irradiance shows that the experimental location is rich in solar energy with a peak of 910 W/m^2 resulting in higher PV module operating temperature attained due to high ambient temperature. Following pre-summer, the performance of the PCMs integration with PV module shows a similar trend owing to the high solar irradiance. Such as in the early period of the experimentation, PCM1 cooled the PV module in higher order, the further rising solar irradiance directly increased the PV module operating temperature, and the cooling effect decreased for PCM1-integrated PV module due to low melting temperature. At 09:00, PCM4 started cooling the PV module temperature higher than other PCMs, and following that, throughout the experimentation period, PCM4 enhanced the cooling effect in higher-order; however, PCM3 exhibits a similar performance to PCM4. During the effective sunshine hours, PV-noPCM, PV-PCM1, PV-PCM2, PV-PCM3 and PV-PCM4 maintained the operating temperature of 71.12 °C, 62.89 °C, 58.90 °C, 56.47 °C and 54.11 °C, respectively. Notably, the period during May shows a peak irradiance of 882.95 W/m^2, and the corresponding PV module performances are similar to that of April. PCM delivers the cooling effect throughout the experimentation period with a peak cooling of 4.3 °C, 8.84 °C, 11.36 °C, and 13.48 °C for PV-PCM1, PV-PCM2, PV-PCM3, and PV-PCM4, respectively.

(a)

(b)

Figure 3. Solar irradiance and thermal profile of PV with and without PCM for (**a**) April and (**b**) May.

3.1.3. Post-Summer

For the experimental location, June and July are considered post-summer and the PCM operations under post-summer are shown in Figure 4a,b, respectively. The monthly average for June shows the peak solar irradiance of 823.02 W/m² due to the season change. Following pre-summer and summer, in this case, PCM1 gained a higher cooling effect; however, the cooling effect failed for a longer period. Notably, PV-noPCM reached the peak operating temperature of 62.07 °C which is lower than in summer, resulting in PCM3 delivering a higher cooling rate than PCM4. It is found that PCM melting temperature plays a vital role in removing the heat from the PV module. From 11:00, PCM3 exhibits a higher cooling rate of ca. 2 °C as compared to PCM4 until the end of experimentation. PCM1 and PCM2 integrated PV module operating temperatures followed a similar pattern

of pre-summer and summer. The reason behind this lower cooling rate for PCM1 and PCM2 is due to high ambient temperature. An increase in ambient temperature influenced the creation of the resistance in the PCM discharging process as the ambient temperature is higher than the PCM melting temperature. Comparatively, July's monthly average PV module with and without PCM operations are similar to June's, as it is also considered post-summer. The peak PV module operating temperature without PCM reached 62.07 °C and the corresponding PCM1, PCM2, PCM3, and PCM4 integrated PV module operating temperatures were reduced by 7.51 °C, 8.87 °C, 13.08 °C, and 11.09 °C, respectively.
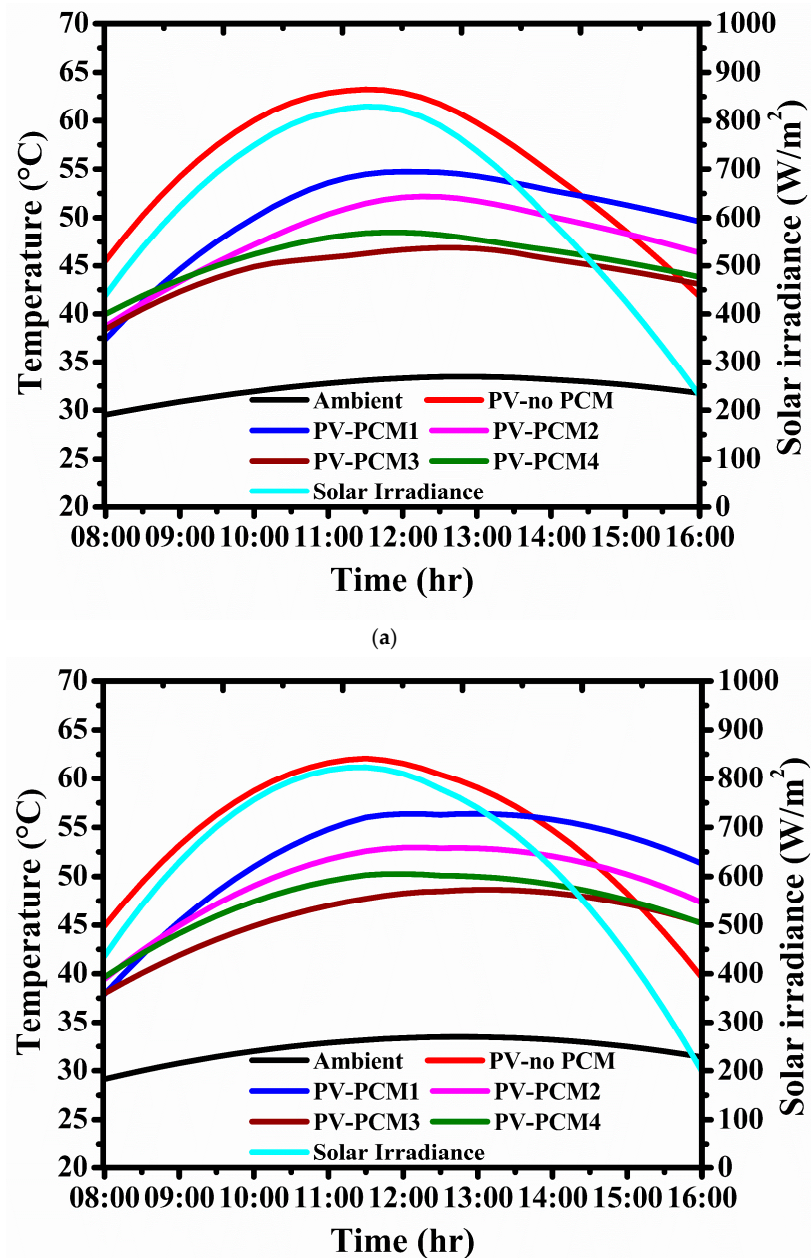
Figure 4. Solar irradiance and thermal profile of PV with and without PCM for (**a**) June and (**b**) July.

3.1.4. Pre-Monsoon and Monsoon

The experiment is performed in a coastal area and August and September are considered pre-monsoon with a periodic rainy day. However, the peak solar irradiance of August and September reached 770.65 W/m^2 and 784.61 W/m^2, as shown in Figure 5a,b, and the corresponding PV-noPCM operating temperature reached 61.09 °C and 61.21 °C, respectively. Following post-summer, PCM3 improved the heat transfer rate between the

PV module and PCM in pre-monsoon because the ambient temperature is low, which favors increasing the heat dissipation between PCM and surroundings. During August, PCM2 increased the cooling rate following PCM3 as compared to PCM1 and PCM4. However, in September, solar irradiance and ambient temperature are lower than in August which makes PCM2 cool the PV module operating temperature in higher order. October and November are considered a typical and clear monsoon period with a peak solar irradiance of 775.14 W/m^2 and 712.97 W/m^2, respectively, as shown in Figure 5c,d, respectively. During November, PCM2 and PCM1 integrated PV modules enhanced the cooling effect greatly as compared to PCM4. Notably, PV-noPCM operating temperature reached 52.08 °C and the corresponding PCM1, PCM2, PCM3, and PCM4 installed PV modules sustained at the temperature of 40.03 °C, 40.35 °C, 41.71 °C, and 43.35 °C, respectively.
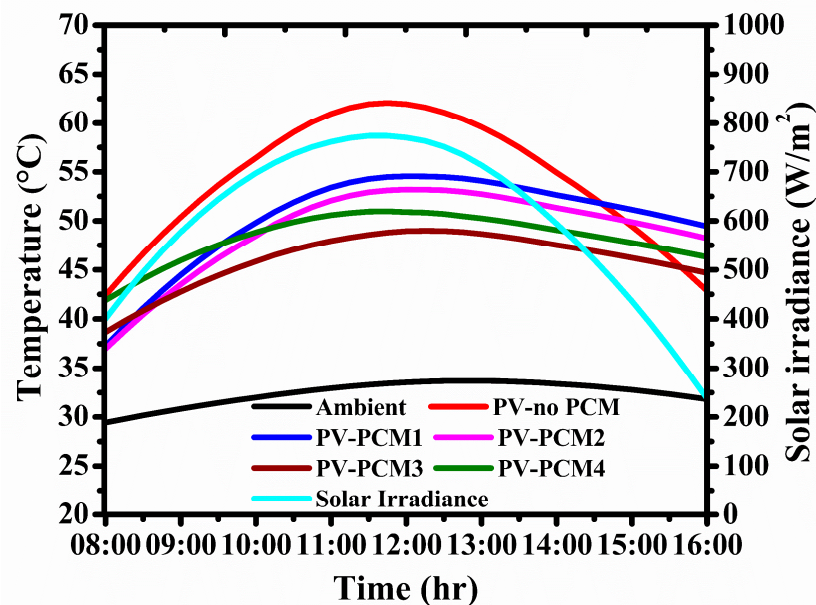
(a)
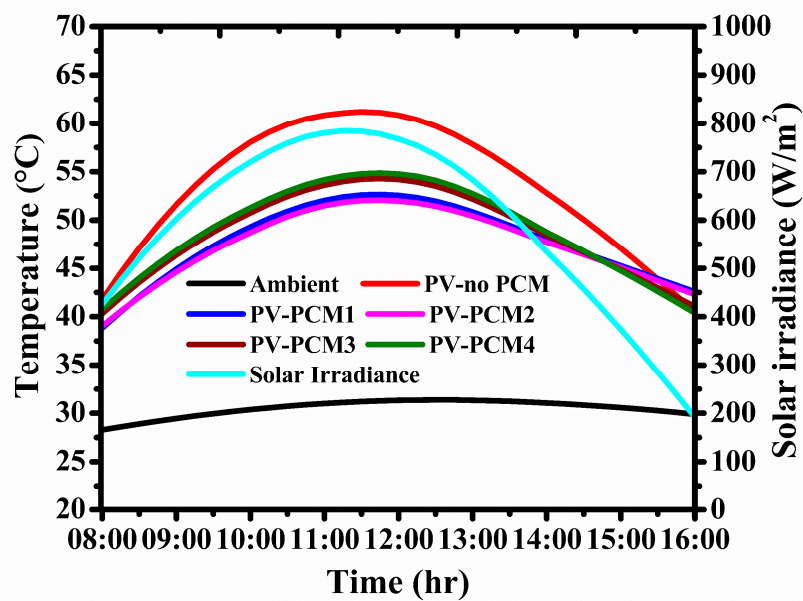
(b)

Figure 5. *Cont.*
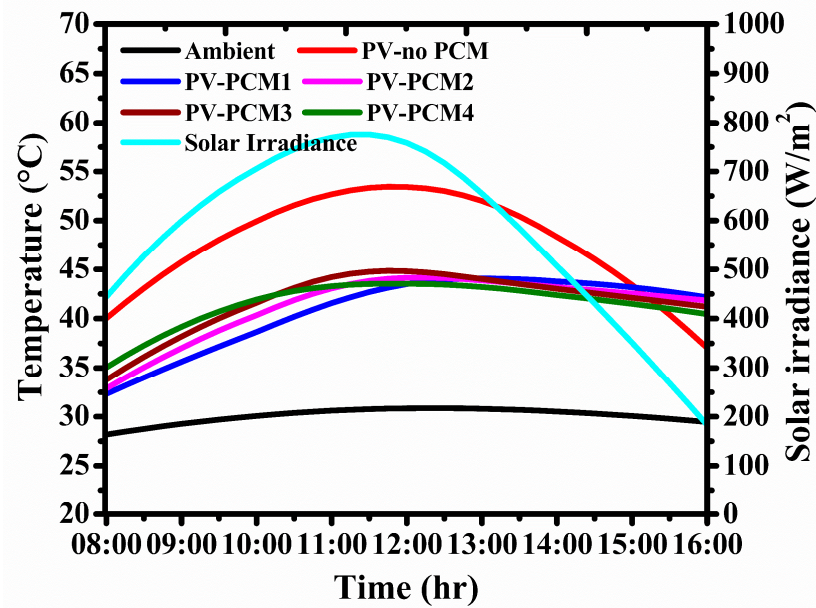
(c)
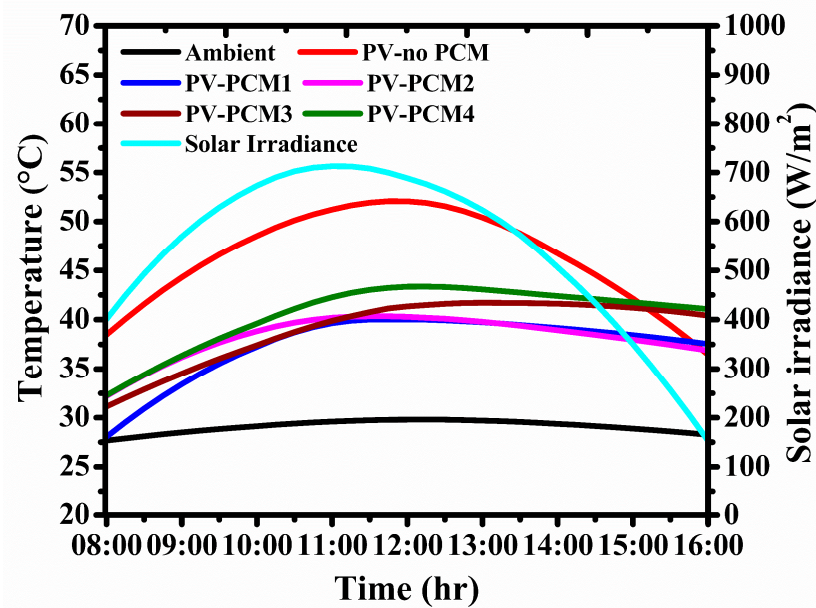
(d)

Figure 5. Solar irradiance and thermal profile of PV with and without PCM for (**a**) August (pre-monsoon), (**b**) September (pre-monsoon), (**c**) October (monsoon), and (**d**) November (monsoon).

3.1.5. Winter and Post-Winter

Following the monsoon, the season turns to winter as the experimental location is above the equatorial belt and it does not snow during the winter. In this case, December and January are considered typical winter seasons for Chidambaram, Tamil Nadu, India. Notably, December and January's ambient temperature is much lower than in other months. A clear sky with lower ambient temperature maintained the lower PV module operating temperature as compared to summer. A selective day's peak solar irradiance in December and January reached 773.97 W/m² and 775.14 W/m², as shown in Figures 6a and 6b, respectively. Comparatively, solar irradiances are higher than in the pre-monsoon and monsoon periods, but the PV module operating temperatures are lower owing to the low ambient temperature. Notably, during January ambient temperatures are moderately higher than in December and the corresponding average PV module temperatures for

no-PCM, PCM1, PCM2, PCM3, and PCM4 are maintained at 50.02 °C, 42.93 °C, 42.04 °C, 43.64 °C, and 44.37 °C, respectively. Due to a lower PV module operating temperature, PCM4 and PCM3 failed to remove the higher amount of heat from the PV module; however, it carries out the cooling effect at a minor rate as compared to PCM1 and PCM2. For the experimental location, February is considered post-winter and the ambient temperature lies around 29–31 °C, as shown in Figure 6c. Notably, the post-winter period performs similarly to winter and the peak PV module operating temperature cooled to 47.01 °C, 46.49 °C, 48.05 °C, and 48.54 for PCM1, PCM2, PCM3, and PCM4, respectively.

(a)

(b)

Figure 6. *Cont.*

(**c**)
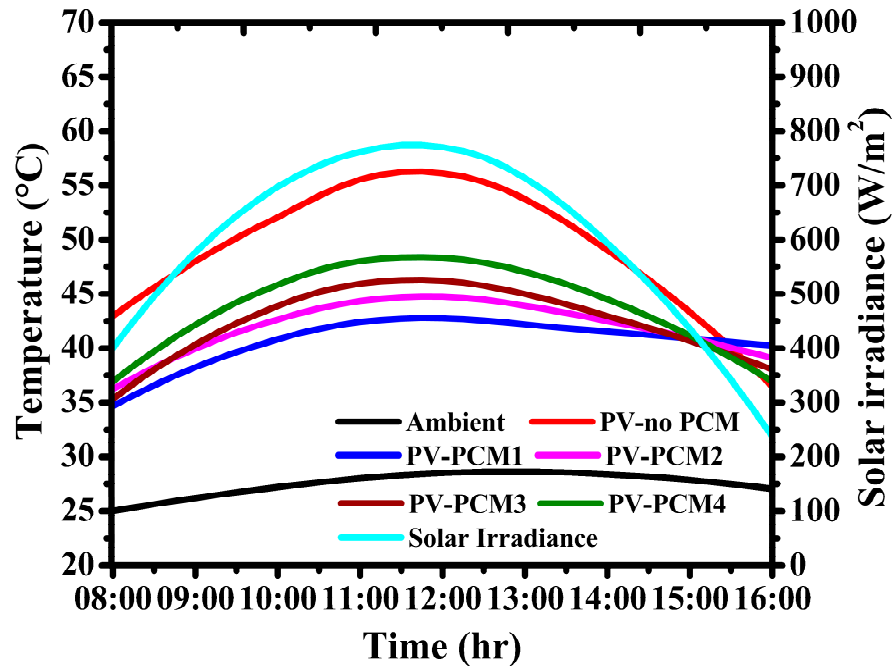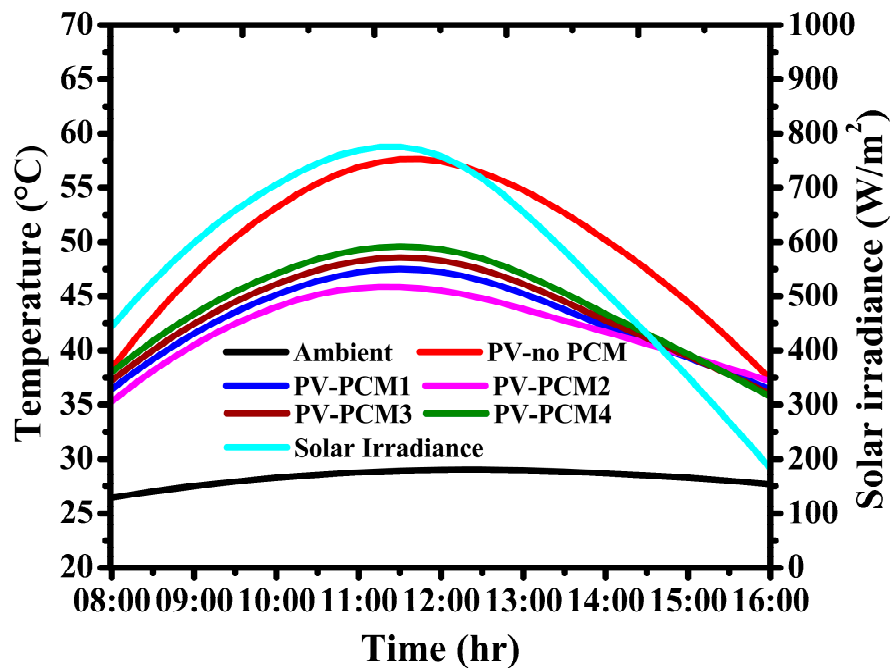
Figure 6. Solar irradiance and thermal profile of PV with and without PCM for (**a**) December (Winter), (**b**) January (Winter), and (**c**) February (post-winter).

3.1.6. Discussion of PCM Influence in Cooling the PV Module

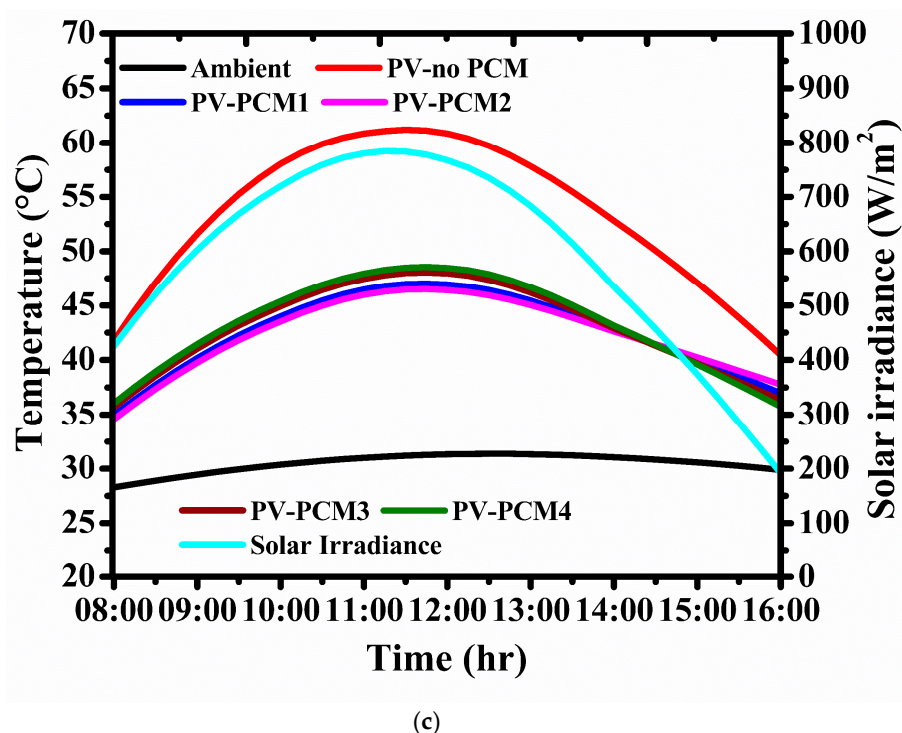Overall, it is found that the PCMs are the predominant cooling agent for tropical climatic conditions; however, several operational complications are raised during the year-round performance. Table 4 shows the summarized year-round thermal performance of the PV-noPCM and PV-PCM along with the solar irradiance and ambient temperature. Notably, during the summer, PCM4 and PCM3 enhanced the heat transfer between the PV module and PCM because the higher melting temperature of the PCM favors removing the higher heat from the PV module and vice versa discharges the stored heat energy to the surroundings. The reason behind the failure of PCM1 and PCM2 during the summer is that PCM was able to remove the heat energy from the PV module in the early period of the sunshine, but failed to dissipate the stored heat energy to the surroundings due to the lower melting temperature of the PCM. This results in PCM1 and PCM2 turning to liquid in the early period of experimentation and the PV module cooling effects are less than PCM3 and PCM4. To eliminate this operational complication with PCM1 and PCM2 during the summer, the thickness/quantity of the PCM container must be increased to maintain the PCM at a latent heat state; however, it could add economic complexity.

Table 4. Year-round PV module thermal profile and meteorological data.

	PV-noPCM (°C)	PV-PCM1 (°C)	PV-PCM2 (°C)	PV-PCM3 (°C)	PV-PCM4 (°C)	Ambient (°C)	Solar Irradiance (W/m^2)
			March (Pre-summer)				
Average	57.74	51.91	49.59	46.61	46.33	32.80	635.78
Peak	66.17	57.31	54.07	50.58	49.83	33.91	815.51
			April (Summer)				
Average	63.29	57.85	54.44	52.88	51.07	32.98	723.86
Peak	71.12	62.89	58.90	56.47	54.11	34.39	914.72

Table 4. *Cont.*

	PV-noPCM (°C)	PV-PCM1 (°C)	PV-PCM2 (°C)	PV-PCM3 (°C)	PV-PCM4 (°C)	Ambient (°C)	Solar Irradiance (W/m²)
			May (Summer)				
Average	61.06	59.00	55.10	53.46	51.89	32.55	690.83
Peak	68.45	64.15	59.61	57.09	54.97	33.57	882.95
			June (Post-summer)				
Average	54.34	50.32	49.12	46.12	48.36	32.45	604.05
Peak	62.07	54.56	53.20	48.99	50.98	33.71	773.97
			July (Post-summer)				
Average	54.71	52.18	49.55	45.90	47.48	32.27	635.35
Peak	62.07	56.39	52.96	48.64	50.27	33.48	823.02
			August (Pre-monsoon)				
Average	53.22	49.29	48.11	45.20	47.39	31.80	592.18
Peak	61.09	53.67	52.33	48.33	50.04	33.09	770.65
			September (Pre-monsoon)				
Average	53.57	47.82	47.47	48.75	49.09	30.50	591.77
Peak	61.21	52.65	52.07	54.29	54.85	31.37	784.61
			October (Monsoon)				
Average	47.86	40.89	41.37	41.86	41.54	30.11	577.83
Peak	53.45	44.07	44.16	44.84	43.54	30.87	775.14
			November (Monsoon)				
Average	46.46	37.49	38.28	39.12	40.61	29.10	545.98
Peak	52.08	40.03	40.35	41.71	43.35	29.81	712.97
			December (Winter)				
Average	49.53	40.74	42.02	42.62	44.13	27.58	604.05
Peak	56.29	42.80	44.77	46.29	48.37	28.65	773.97
			January (Winter)				
Average	50.02	42.93	42.04	43.64	44.37	28.30	577.83
Peak	57.66	47.52	45.87	48.56	49.60	29.30	775.14
			February (Post-winter)				
Average	53.57	42.59	42.36	43.14	43.44	30.50	591.77
Peak	61.21	47.01	46.49	48.05	48.54	31.37	784.65

3.2. PV Module Electrical Profile

PV module electrical profiles are indirectly proportional to their operating temperature. It is well known that an increase in solar irradiance can produce a higher current as a solar cell is a current generator; however, an increase in irradiance directly increases the PV module operating temperature resulting in voltage drops and it affects the power profile. Figure 7 shows the monthly average power production of PV-noPCM, PV-PCM1, PV-PCM2, PV-PCM3, and PV-PCM4. It is found that summer yields higher power production for PCM4 and PCM3 and during winter, PCM1 and PCM2 attained higher power production.

Table 5 shows the average and peak annual profile for power, performance ratio (PR), efficiency, and the corresponding capacity utilization factor. Notably, the electrical profile of the PV-noPCM, PV-PCM1, PV-PCM2, PV-PCM3, and PV-PCM4 follows a similar trend of thermal profile. An appropriate PCM melting temperature enhanced the higher power extraction; for example, during January, PV-PCM2 produced the higher average power and peak power, PR, η, and CUF, as compared to other PV-PCMs and PV-noPCM. Notably, during March and April, PV-PCM3 and PV-PCM4 performances are more effective than PV-PCM2 due to the PCM melting at an early stage. PCM operations are mainly related to the environmental conditions at the experimental site, such as an increase in ambient temperature makes PCM1 and PCM 2 not suitable for summer and pre-monsoon conditions. As mentioned earlier, stored heat energy from the PCM container failed to dissipate the

higher amount of heat energy to the surroundings. Following those other months, a significant difference in the electrical profile is noted, which shows that the PCM melting temperature plays a significant role in enhancing the PV module performance. Overall, it is found that higher power production is achieved for April, but higher efficiency and PR are achieved for winter due to a higher PV module operating temperature. However, the CUF follows the PV module power production resulting in a higher CUF recorded for April.
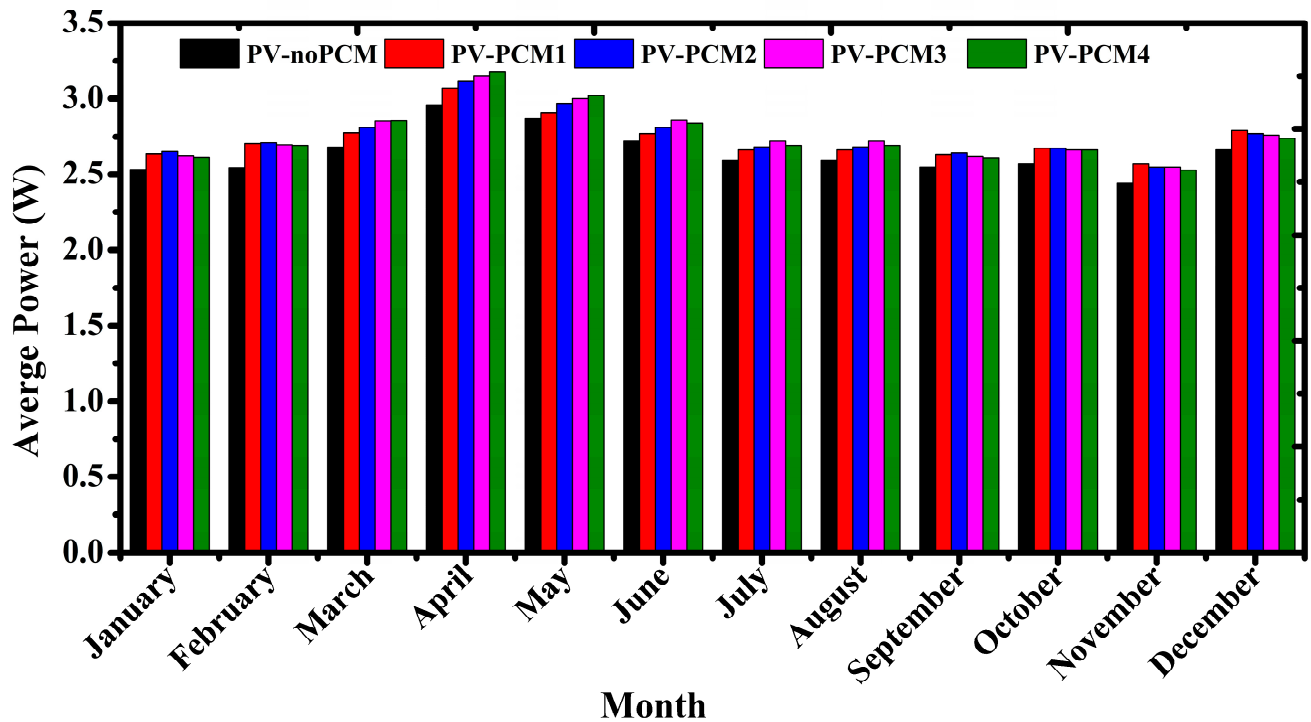

Figure 7. Monthly average power production for PV-noPCM, PV-PCM1, PV-PCM2, PV-PCM3, and PV-PCM4.

Table 5. Electrical profile of PV-noPCM, PV-PCM1, PV-PCM2, PV-PCM3, and PV-PCM4.

	Average Power (W)	Peak Power (W)	Average PR (%)	Peak PR (%)	Average η (%)	Peak η (%)	CUF
			January (Winter)				
PV-noPCM	2.53	3.30	88.46	94.14	12.80	13.19	16.89
PV-PCM1	2.63	3.47	91.64	94.55	12.43	12.67	17.56
PV-PCM2	2.65	3.50	92.04	95.06	12.38	12.58	17.66
PV-PCM3	2.62	3.45	91.32	94.73	12.46	12.72	17.49
PV-PCM4	2.61	3.44	90.99	94.85	12.50	12.67	17.42
			February (Post-winter)				
PV-noPCM	2.55	3.28	86.86	92.75	12.98	13.37	16.97
PV-PCM1	2.70	3.53	91.79	95.22	12.41	12.64	18.03
PV-PCM2	2.71	3.54	91.89	95.38	12.40	12.61	18.06
PV-PCM3	2.70	3.51	91.54	94.89	12.44	12.69	17.97
PV-PCM4	2.69	3.50	91.41	94.87	12.45	12.64	17.93
			March (Pre-summer)				
PV-noPCM	2.68	3.32	85.00	91.20	13.19	13.63	17.85
PV-PCM1	2.78	3.47	87.61	95.52	12.89	13.17	18.51
PV-PCM2	2.81	3.53	88.65	94.63	12.77	13.00	18.73
PV-PCM3	2.85	3.60	89.99	94.86	12.62	12.82	19.02
PV-PCM4	2.86	3.61	90.11	93.25	12.60	13.17	19.05

Table 5. *Cont.*

	Average Power (W)	Peak Power (W)	Average PR (%)	Peak PR (%)	Average η (%)	Peak η (%)	CUF
			April (Summer)				
PV-noPCM	2.96	3.63	82.51	88.50	13.48	13.89	19.75
PV-PCM1	3.07	3.80	84.95	92.69	13.20	13.46	20.44
PV-PCM2	3.12	3.88	86.47	92.57	13.02	13.25	20.82
PV-PCM3	3.15	3.93	87.18	91.37	12.94	13.13	21.00
PV-PCM4	3.18	3.98	87.99	91.01	12.85	13.46	21.20
			May (Summer)				
PV-noPCM	2.87	3.57	83.51	89.74	13.37	13.75	19.10
PV-PCM1	2.91	3.65	84.43	92.32	13.26	13.53	19.39
PV-PCM2	2.97	3.74	86.18	92.35	13.06	13.29	19.81
PV-PCM3	3.00	3.79	86.91	91.15	12.97	13.16	19.98
PV-PCM4	3.02	3.83	87.62	90.69	12.89	13.53	20.15
			June (Post-summer)				
PV-noPCM	2.59	3.22	86.52	91.87	13.02	13.42	17.29
PV-PCM1	2.66	3.35	88.32	94.18	12.81	13.03	17.73
PV-PCM2	2.68	3.37	88.86	94.30	12.75	12.96	17.84
PV-PCM3	2.72	3.45	90.21	93.55	12.59	12.74	18.13
PV-PCM4	2.69	3.41	89.20	92.10	12.71	13.03	17.92
			July (Post-summer)				
PV-noPCM	2.72	3.42	86.35	93.13	13.04	13.42	18.12
PV-PCM1	2.77	3.54	87.49	93.89	12.91	13.12	18.48
PV-PCM2	2.81	3.60	88.67	93.20	12.77	12.95	18.73
PV-PCM3	2.86	3.69	90.30	93.85	12.58	12.72	19.10
PV-PCM4	2.84	3.64	89.60	93.10	12.66	13.12	18.93
			August (Pre-monsoon)				
PV-noPCM	2.56	3.22	87.02	91.91	12.96	13.37	17.05
PV-PCM1	2.62	3.35	88.78	94.24	12.76	12.98	17.47
PV-PCM2	2.64	3.37	89.31	94.00	12.70	12.91	17.58
PV-PCM3	2.68	3.44	90.62	93.70	12.55	12.71	17.85
PV-PCM4	2.65	3.41	89.64	92.34	12.66	12.98	17.66
			September (Pre-monsoon)				
PV-noPCM	2.55	3.28	86.86	92.75	12.98	13.37	16.97
PV-PCM1	2.63	3.43	89.44	93.48	12.68	12.93	17.56
PV-PCM2	2.64	3.44	89.60	93.38	12.66	12.90	17.60
PV-PCM3	2.62	3.40	89.03	92.81	12.73	13.02	17.46
PV-PCM4	2.61	3.39	88.88	92.78	12.75	12.93	17.42
			October (Monsoon)				
PV-noPCM	2.57	3.37	89.43	94.28	12.68	12.97	17.11
PV-PCM1	2.67	3.56	92.55	96.39	12.32	12.49	17.83
PV-PCM2	2.67	3.54	92.34	96.14	12.35	12.49	17.77
PV-PCM3	2.66	3.52	92.12	95.74	12.37	12.53	17.72
PV-PCM4	2.66	3.54	92.26	95.17	12.36	12.49	17.75
			November (Monsoon)				
PV-noPCM	2.44	3.13	90.05	94.54	12.61	12.90	16.29
PV-PCM1	2.57	3.32	94.08	98.31	12.15	12.28	17.10
PV-PCM2	2.55	3.31	93.72	96.45	12.19	12.29	17.03
PV-PCM3	2.55	3.32	93.34	96.93	12.23	12.36	16.99
PV-PCM4	2.53	3.28	92.68	96.41	12.31	12.28	16.85
			December (Winter)				
PV-noPCM	2.66	3.31	88.68	94.53	12.77	13.12	17.73
PV-PCM1	2.79	3.55	92.62	95.34	12.31	12.42	18.62
PV-PCM2	2.77	3.52	92.05	94.64	12.38	12.52	18.49
PV-PCM3	2.76	3.49	91.78	95.05	12.41	12.60	18.42
PV-PCM4	2.74	3.45	91.10	94.33	12.49	12.42	18.26

4. Conclusions

The PCM-assisted PV module cooling technique was demonstrated to find the suitable PCM melting temperature for annual performance enhancement. It was found that PCM melting temperature plays a crucial role in removing the heat from the PV module, as well as in dissipating the heat from the PCM container to the surroundings. During summer, the highest cooling was achieved for April with a difference of 17.14 °C with the help of PCM4. Comparatively, the same PCM4 failed to achieve a higher cooling effect in winter due to inappropriate PCM melting. Overall, a lower cooling rate is achieved for winter and monsoon seasons because lower ambient temperature favors cooling the PV module naturally. However, the PR and efficiency of the PV modules are higher in the winter and monsoon periods owing to the low operating temperature. Further, it is concluded that suggesting a single melting temperature of PCM for cooling the PV module is not appropriate year-round under tropical climatic conditions. It is recommended to incorporate dual PCM containers, such as a cascaded structure, for year-round PV module cooling.

References

1. Quang, D.V.; Milani, D.; Zahra, M.A. A review of potential routes to zero and negative emission technologies via the integration of renewable energies with CO_2 capture processes. *Int. J. Greenh. Gas Control* **2023**, *124*, 103862. [CrossRef]
2. Kolsi, L.; Al-Dahidi, S.; Kamel, S.; Aich, W.; Boubaker, S.; Ben Khedher, N. Prediction of Solar Energy Yield Based on Artificial Intelligence Techniques for the Ha'il Region, Saudi Arabia. *Sustainability* **2022**, *15*, 774. [CrossRef]
3. Fathi, T.; Jouini, H.; Mami, A.; Ben Khedher, N.; Aich, W.; Boudjemline, A.; Boujelbene, M. Comparative Assessment between Five Control Techniques to Optimize the Maximum Power Point Tracking Procedure for PV Systems. *Mathematics* **2022**, *10*, 1080.
4. Ang, T.-Z.; Salem, M.; Kamarol, M.; Das, H.; Nazari, M.; Prabaharan, N. A comprehensive study of renewable energy sources: Classifications, challenges and suggestions. *Energy Strategy Rev.* **2022**, *43*, 100939. [CrossRef]
5. Alharthi, M.; Hanif, I.; Alamoudi, H. Impact of environmental pollution on human health and financial status of households in MENA countries: Future of using renewable energy to eliminate the environmental pollution. *Renew. Energy* **2022**, *190*, 338–346. [CrossRef]
6. Pouladian-Kari, A.; Eslami, S.; Tadjik, A.; Kirchner, L.; Pouladian-Kari, R.; Golshanfard, A. A novel solution for addressing the problem of soiling and improving performance of PV solar systems. *Sol. Energy* **2022**, *241*, 315–326. [CrossRef]
7. Abenante, L. Analytical modeling of reversible performance loss of PV modules and module arrays. *Sol. Energy* **2022**, *239*, 375–387. [CrossRef]
8. Chiang, W.; Permana, I.; Wang, F.; Chen, H.; Erdenebayar, M. Experimental investigation for an innovative hybrid photovoltaic/Thermal (PV/T) solar system. *Energy Rep.* **2022**, *8*, 910–918. [CrossRef]
9. Durganjali, C.S.; Avinash, G.; Megha, K.; Ponnalagu, R.; Goel, S.; Radhika, S. Prediction of PV cell parameters at different temperatures via ML algorithms and comparative performance analysis in Multiphysics environment. *Energy Convers. Manag.* **2023**, *282*, 116881. [CrossRef]
10. Moharram, K.A.; Abd-Elhady, M.; Kandil, H.; El-Sherif, H. Enhancing the performance of photovoltaic panels by water cooling. *Ain Shams Eng. J.* **2013**, *4*, 869–877. [CrossRef]
11. Moradi, K.; Ali Ebadian, M.; Lin, C.-X. A review of PV/T technologies: Effects of control parameters. *Int. J. Heat Mass Transf.* **2013**, *64*, 483–500. [CrossRef]
12. Moradgholi, M.; Nowee, S.; Abrishamchi, I. Application of heat pipe in an experimental investigation on a novel photovoltaic/thermal (PV/T) system. *Sol. Energy* **2014**, *107*, 82–88. [CrossRef]
13. Fudholi, A.; Sopian, K.; Yazdi, M.; Ruslan, M.; Ibrahim, A.; Kazem, H. Performance analysis of photovoltaic thermal (PVT) water collectors. *Energy Convers. Manag.* **2014**, *78*, 641–651. [CrossRef]

14. Kumar, A.; Baredar, P.; Qureshi, U. Historical and recent development of photovoltaic thermal (PVT) technologies. *Renew. Sustain. Energy Rev.* **2015**, *42*, 1428–1436. [CrossRef]

15. Lamnatou, C.; Chemisana, D. Photovoltaic/thermal (PVT) systems: A review with emphasis on environmental issues. *Renew. Energy* **2017**, *105*, 270–287. [CrossRef]

16. Mostakim, K.; Hasanuzzaman, M. Global prospects, challenges and progress of photovoltaic thermal system. *Sustain. Energy Technol. Assess.* **2022**, *53*, 102426. [CrossRef]

17. Chandrasekar, M.; Senthilkumar, T. Five decades of evolution of solar photovoltaic thermal (PVT) technology—A critical insight on review articles. *J. Clean. Prod.* **2021**, *322*, 128997. [CrossRef]

18. Velmurugan, K.; Kumarasamy, S.; Wongwuttanasatian, T.; Seithtanabutara, V. Review of PCM types and suggestions for an applicable cascaded PCM for passive PV module cooling under tropical climate conditions. *J. Clean. Prod.* **2021**, *293*, 126065. [CrossRef]

19. Velmurugan, K.; Elavarasan, R.M.; Van De, P.; Karthikeyan, V.; Korukonda, T.B.; Dhanraj, J.A.; Emsaeng, K.; Chowdhury, M.S.; Techato, K.; El Khier, B.S.A.; et al. A Review of Heat Batteries Based PV Module Cooling—Case Studies on Performance Enhancement of Large-Scale Solar PV System. *Sustainability* **2022**, *14*, 1963. [CrossRef]

20. Abed, A.; Mouziraji, H.; Bakhshi, J.; Dulaimi, A.; Mohammed, H.; Ibrahem, R.; Ben Khedher, N.; Yaïci, W.; Mahdi, J. Numerical analysis of the energy-storage performance of a PCM-based triplex-tube containment system equipped with arc-shaped fins. *Front. Chem.* **2022**, *10*, 1057196. [CrossRef]

21. Ma, T.; Li, Z.; Zhao, J. Photovoltaic panel integrated with phase change materials (PV-PCM): Technology overview and materials selection. *Renew. Sustain. Energy Rev.* **2019**, *116*, 109406. [CrossRef]

22. Ali, H.M. Recent advancements in PV cooling and efficiency enhancement integrating phase change materials based systems—A comprehensive review. *Solar Energy* **2020**, *197*, 163–198. [CrossRef]

23. Rekha, S.M.S.; Karthikeyan, V.; Thuy, L.T.; Binh, Q.; Techato, K.; Kannan, V.; Roy, V.; Sukchai, S.; Velmurugan, K. Efficient heat batteries for performance boosting in solar thermal cooking module. *J. Clean. Prod.* **2021**, *324*, 129223. [CrossRef]

24. Fikri, M.A.; Samykano, M.; Pandey, A.; Kadirgama, K.; Kumar, R.; Selvaraj, J.; Rahim, N.; Tyagi, V.; Sharma, K.; Saidur, R. Recent progresses and challenges in cooling techniques of concentrated photovoltaic thermal system: A review with special treatment on phase change materials (PCMs) based cooling. *Sol. Energy Mater. Sol. Cells* **2022**, *241*, 111739. [CrossRef]

25. Preet, S. A review on the outlook of thermal management of photovoltaic panel using phase change material. *Energy Clim. Change* **2021**, *2*, 100033. [CrossRef]

26. Velmurugan, K.; Karthikeyan, V.; Korukonda, T.; Poongavanam, P.; Nadarajan, S.; Kumarasamy, S.; Wongwuttanasatian, T.; Sandeep, D. Experimental studies on photovoltaic module temperature reduction using eutectic cold phase change material. *Solar Energy* **2020**, *209*, 302–315. [CrossRef]

27. Velmurugan, K.; Karthikeyan, V.; Kumarasamy, S.; Wongwuttanasatian, T.; Sa-ngiamsak, C. Thermal mapping of photovoltaic module cooling via radiation-based phase change material matrix: A case study of a large-scale solar farm in Thailand. *J. Energy Storage* **2022**, *55*, 105805. [CrossRef]

28. Lim, J.-H.; Lee, Y.-S.; Seong, Y.-B. Diurnal Thermal Behavior of Photovoltaic Panel with Phase Change Materials under Different Weather Conditions. *Energies* **2017**, *10*, 1983. [CrossRef]

29. Prasannaa, P.; Ramkumar, R.; Sunilkumar, K.; Rajasekar, R. Experimental study on a binary mixture ratio of fatty acid-based PCM integrated to PV panel for thermal regulation on a hot and cold month. *Int. J. Sustain. Energy* **2021**, *40*, 218–234. [CrossRef]

30. Klugmann-Radziemska, E.; Wcisło-Kucharek, P. Photovoltaic module temperature stabilization with the use of phase change materials. *Sol. Energy* **2017**, *150*, 538–545. [CrossRef]

31. Mahamudul, H.; Rahman, M.; Metselaar, H.; Mekhilef, S.; Shezan, S.; Sohel, R.; Karim, S.A.; Badiuzaman, W. Temperature Regulation of Photovoltaic Module Using Phase Change Material: A Numerical Analysis and Experimental Investigation. *Int. J. Photoenergy* **2016**, *2016*, 5917028. [CrossRef]

32. Khedher, N.B.; Mahdi, J.; Majdi, H.; Al-Azzawi, W.; Dhahbi, S.; Talebizadehsardari, P. A hybrid solidification enhancement in a latent-heat storage system with nanoparticles, porous foam, and fin-aided foam strips. *J. Energy Storage* **2022**, *56*, 106070. [CrossRef]

33. Ben Khedher, N.; Bantan, R.; Kolsi, L.; Omri, M. Performance investigation of a vertically configured LHTES via the combination of nano-enhanced PCM and fins: Experimental and numerical approaches. *Int. Commun. Heat Mass Transf.* **2022**, *137*, 106246. [CrossRef]

34. Ben Khedher, N.; Mehryan, S.A.M. Study of tree-shaped optimized fins in a heat sink filled by solid-solid nanocomposite phase change material. *Int. Commun. Heat Mass Transf.* **2022**, *136*, 106195. [CrossRef]

35. Karthikeyan, V.; Sirisamphanwong, C.; Sukchai, S.; Sahoo, S.; Wongwuttanasatian, T. Reducing PV module temperature with radiation based PV module incorporating composite phase change material. *J. Energy Storage* **2020**, *29*, 101346. [CrossRef]

36. Li, X.; Cui, W.; Simon, T.; Ma, T.; Cui, T.; Wang, Q. Pore-scale analysis on selection of composite phase change materials for photovoltaic thermal management. *Appl. Energy* **2021**, *302*, 117558. [CrossRef]

37. Abdulmunem, A.R.; Samin, P.; Rahman, H.; Hussien, H.; Ghazali, H. A novel thermal regulation method for photovoltaic panels using porous metals filled with phase change material and nanoparticle additives. *J. Energy Storage* **2021**, *39*, 102621. [CrossRef]

38. Arıcı, M.; Bilgin, F.; Nižetić, S.; Papadopoulos, A. Phase change material based cooling of photovoltaic panel: A simplified numerical model for the optimization of the phase change material layer and general economic evaluation. *J. Clean. Prod.* **2018**, *189*, 738–745. [CrossRef]

39. Elavarasan, R.M.; Velmurugan, K.; Subramaniam, U.; Kumar, A.; Almakhles, D. Experimental Investigations Conducted for the Characteristic Study of OM29 Phase Change Material and Its Incorporation in Photovoltaic Panel. *Energies* **2020**, *13*, 897. [CrossRef]

40. Rashwan, S.S.; Shaaban, A.; Al-Suliman, F. A comparative study of a small-scale solar PV power plant in Saudi Arabia. *Renew. Sustain. Energy Rev.* **2017**, *80*, 313–318. [CrossRef]

41. Srivastava, R.; Tiwari, A.; Giri, V. An overview on performance of PV plants commissioned at different places in the world. *Energy Sustain. Dev.* **2020**, *54*, 51–59. [CrossRef]

42. Hasan, A.; Sarwar, J.; Alnoman, H.; Abdelbaqi, S. Yearly energy performance of a photovoltaic-phase change material (PV-PCM) system in hot climate. *Solar Energy* **2017**, *146*, 417–429. [CrossRef]

43. Pluss®. Available online: https://pluss.co.in/save-pcms-product-range/ (accessed on 4 April 2023).